Thrombin Inhibition by Novel Benzamidine Derivatives: A Free-Energy Perturbation Study

Cristiano Ruch Werneck Guimarães*,§ and Ricardo Bicca de Alencastro

Physical Organic Chemistry Group, Departamento de Química Orgânica, Instituto de Química, Universidade Federal do Rio de Janeiro, Cidade Universitária, CT, Bloco A, lab. 609, Rio de Janeiro, RJ 21949-900, Brazil

Thrombin is a serine protease responsible for blood coagulation. Since thrombin inhibitors appear to be effective in the treatment and prevention of thrombotic and embolic disorders, considerable attention has been focused on the structure and interactions of this enzyme. In this work, to evaluate the relative free energies of hydration and binding to thrombin for some benzamidine derivatives, we used the finite difference thermodynamic integration (FDTI) algorithm within the Discover program of MSI. By this method, two possible orders of hydration for the candidates were obtained: *p*-amidinophenylpyruvate > *p*-(2-oxo-1-propyl)benzamidine > *p*-methylbenzamidine > *p*-ethylbenzamidine > *p*-(1-propyl)benzamidine > benzamidine and *p*-amidinophenylpyruvate > *p*-(2-oxo-1-propyl)benzamidine > *p*-methylbenzamidine > *p*-ethylbenzamidine > benzamidine > *p*-(1-propyl)benzamidine. We also obtained the following order for thrombin binding: *p*-(2-oxo-1-propyl)benzamidine > *p*-ethylbenzamidine > *p*-(1-propyl)benzamidine > *p*-methylbenzamidine > benzamidine > *p*-amidinophenylpyruvate.

Introduction

Clot formation results from a complex sequence of biochemical events that comprise the coagulation cascade, which involves the interaction of specific blood proteins followed by platelet aggregation.[1−3] Although this process occurs in blood vessels to repair minor internal injuries, exaggerated clot formation leads to several cardiovascular disorders such as venous and arterial thrombosis, atrial fibrillation, stroke, and myocardial infarction.[4] Thrombin is a serine protease that plays a central role in the coagulation cascade through the conversion of fibrinogen to fibrin and platelet activation.[5] As the most potent stimulator of platelet aggregation, thrombin has become the principal target in the development of new antithrombotic agents.[6−10]

Thrombin consists of an A chain of 36 amino acids and a B chain of 259 amino acids connected by a disulfide bridge.[11] This enzyme, related to trypsin and chymotrypsin, has the catalytic triad (Asp102−His57−Ser195) characteristic of these serine proteases. Besides the catalytic triad, the active site of thrombin has three other important binding pockets. The S1 pocket, which contains an aspartate (Asp189), a small hydrophobic site called the P-pocket (S2 pocket), defined by the Tyr60A-Pro60B-Pro60C-Trp60D insertion loop, and a larger hydrophobic site called the D-pocket (S3 pocket), which is separated from the P-pocket by the side chain of Leu99.[12]

The *p*-amidinophenylpyruvate (APPA) (K_i = 620 nM)[11,13] and benzamidine (Bz) (K_i = 300 nM)[11,14,15] compounds are examples of thrombin inhibitors (Figure 1). The first one is an electrophilic inhibitor, whose carbonyl group is attacked by the Ser195 residue of the
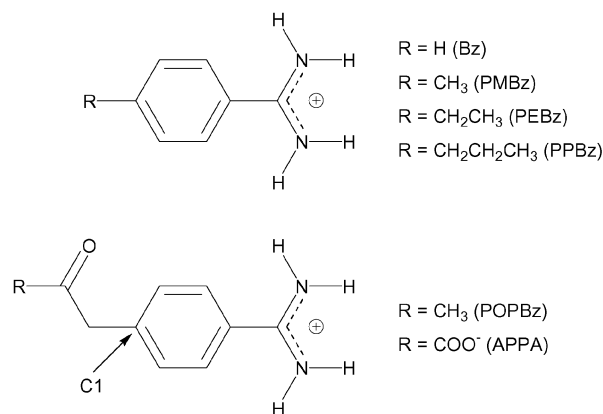

Figure 1. Benzamidine derivatives studied in this work. For the meaning of C1, see computational details.

catalytic triad. The second is a noncovalent inhibitor. When protonated, the amidine group of both APPA and Bz interacts with the active site of thrombin through a salt bridge with the Asp189 residue (S1 pocket).

Many pharmaceutical companies have devoted considerable time and effort toward the development of an orally active synthetic thrombin inhibitor.[16−20] However, despite high in vitro affinity, only a limited oral bioavailability has been obtained because of low intestinal permeability. Low membrane permeability is derived from the presence of highly basic functional groups in most of the synthetic thrombin inhibitors.[21] Thus, the design of more lipophilic compounds is needed to improve the pharmacokinetic profile of thrombin inhibitors. In addition, since the S1 pocket of thrombin contains the Ala190 residue, and the S1 pocket of trypsin contains the Ser190 residue, modifications in the P1 site of thrombin inhibitors, through the use of more lipophilic substituent groups, should help to increase their selectivity for thrombin with respect to trypsin.[8,22,23]

* Corresponding author: Phone: (203) 432-6288. Fax: (203) 432-6144. E-mail:.cris@ramana.chem.yale.edu.
§ Current address: 225 Prospect St., Sterling Chemistry Laboratory, Department of Chemistry, Yale University, New Haven, CT 06520-8107.
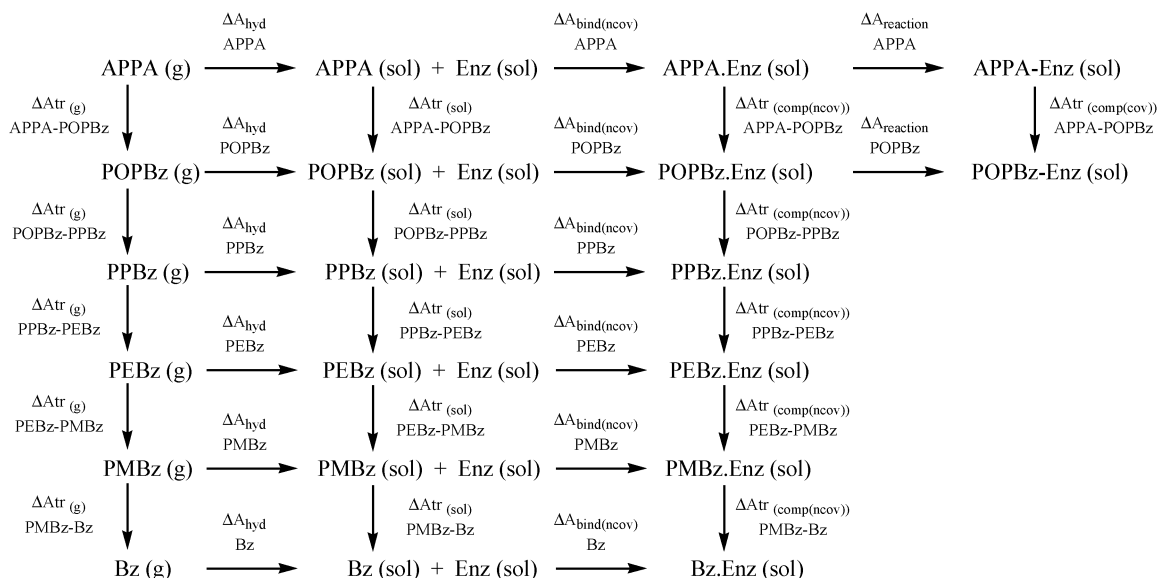
Figure 2. Thermodynamic cycles used for the calculation of relative free energies (see text for details).

Therefore, to improve the binding to thrombin, enhance the selectivity for this enzyme, and increase the intestinal permeability of Bz and APPA, we have added groups with a greater hydrophobicity to the para position of Bz and substituted the carboxylate group of APPA by a methyl group (Figure 1). In Figure 1, PMBz, PEBz, PPBz, and POPBz are *p*-methylbenzamidine, *p*-ethylbenzamidine, *p*-(1-propyl)benzamidine, and *p*-(2-oxo-1-propyl)benzamidine, respectively. In this work, we present only a theoretical analysis of thrombin inhibition by using molecular dynamics (MD) simulations in conjunction with free energy perturbation (FEP) calculations.[24−27] More specifically, we computed the relative free energies of binding to thrombin for the noncovalent candidates, PPBz, PEBz, PMBz, and Bz. Since ketones are only used as reactive functional groups in thrombin inhibitor candidates when activated,[4] it is not entirely clear if POPBz would be an electrophilic inhibitor. Thus, we decided to calculate both the relative free energy of noncovalent binding to thrombin and the relative free energy of reaction with the enzyme between POPBz and APPA. Moreover, to verify the influence of hydration in the binding process, we have also calculated the relative free energies of hydration for these compounds.

Theoretical Background

Considering two states, 1 and 2, the Helmholtz free energy variation between them is given by eq 1. Because of the separation of Q_{NVT}, the Helmholtz free energy variation can be expressed as a sum of ideal gas and configurational parts.

$$\Delta A = -kT \ln \frac{Q2_{NVT}}{Q1_{NVT}} = \Delta A_{\mathrm{id}} - kT \ln \frac{Z2_{NVT}}{Z1_{NVT}} \quad (1)$$

When calculating relative free energy differences, a thermodynamic cycle is generally applied.[28] Here, we have used the thermodynamic cycles exhibited in Figure 2. Since the free energy is a thermodynamic state function, the cycles on the left side of Figure 2 give the relative free energies of hydration

$$\Delta\Delta A_{\mathrm{hyd}} = \Delta A_{\mathrm{hyd}}Y - \Delta A_{\mathrm{hyd}}X =$$
$$\Delta A\mathrm{tr}_{(\mathrm{sol})}(X{\to}Y) - \Delta A\mathrm{tr}_{(\mathrm{g})}(X{\to}Y) \quad (2)$$

where X and Y are any two benzamidine derivatives, ΔA_{hyd} is the absolute free energy of hydration, and $\Delta A\mathrm{tr}_{(\mathrm{sol})}(X{\to}Y)$ and $\Delta A\mathrm{tr}_{(\mathrm{g})}(X{\to}Y)$ are the free energies associated with the transformation of X into Y in the solution and gas phase, respectively. The cycles in the center of Figure 2 give the relative free energies of noncovalent binding

$$\Delta\Delta A_{\mathrm{bind(ncov)}} = \Delta A_{\mathrm{bind(ncov)}}Y - \Delta A_{\mathrm{bind(ncov)}}X =$$
$$\Delta A\mathrm{tr}_{(\mathrm{comp(ncov)})}(X{\to}Y) - \Delta A\mathrm{tr}_{(\mathrm{sol})}(X{\to}Y) \quad (3)$$

where $\Delta A_{\mathrm{bind(ncov)}}$ is the absolute free energy of noncovalent binding, and $\Delta A\mathrm{tr}_{(\mathrm{comp(ncov)})}(X{\to}Y)$ is the free energy associated with the transformation of X into Y inside the noncovalent complex between thrombin and a benzamidine derivative. Finally, the cycle on the right side of Figure 2 gives the relative free energy of reaction with the enzyme between POPBz and APPA

$$\Delta\Delta A_{\mathrm{reaction}} = \Delta A_{\mathrm{reaction}}\mathrm{POPBz} - \Delta A_{\mathrm{reaction}}\mathrm{APPA} =$$
$$\Delta A\mathrm{tr}_{(\mathrm{comp(cov)})}(\mathrm{APPA}{\to}\mathrm{POPBz}) -$$
$$\Delta A\mathrm{tr}_{(\mathrm{comp(ncov)})}(\mathrm{APPA}{\to}\mathrm{POPBz}) \quad (4)$$

where $\Delta A_{\mathrm{reaction}}$ is the absolute free energy of reaction between the enzyme and an electrophilic compound, and $\Delta A\mathrm{tr}_{(\mathrm{comp(cov)})}(\mathrm{APPA}{\to}\mathrm{POPBz})$ is the free energy associated with the transformation of APPA into POPBz inside the covalent complex with thrombin. It is interesting to note that $\Delta\Delta A_{\mathrm{reaction}}$ added to $\Delta\Delta A_{\mathrm{bind(ncov)}}$ between POPBz and APPA gives the relative free energy of covalent binding to thrombin ($\Delta\Delta A_{\mathrm{bind(cov)}}$) for these two compounds.

Because the quantities ΔA_{hyd}, $\Delta A_{\mathrm{bind(ncov)}}$, and $\Delta A_{\mathrm{reaction}}$ are impracticable to compute due to the time scale and the enormous atom reorganization involved in these thermodynamic processes, the relative free energies described above are obtained through the simulation of nonphysical paths transforming one molecule into another in different environments. Therefore, the differ-

ences in ΔA resulting from the kinetic energy, as in eq 1, may be assumed to be identical in calculating, for example, $\Delta A tr_{(sol)}$ and $\Delta A tr_{(g)}$, $\Delta A tr_{(comp(ncov))}$ and $\Delta A tr_{(sol)}$, or $\Delta A tr_{(comp(cov))}$ and $\Delta A tr_{(comp(ncov))}$ (Figure 2). Given that, it is reasonable to suppose that the internal energy is equal to the potential energy $(H - U)$.[27] Thus, the perturbation method (PM) equation[27] may be written as

$$\Delta A = -kT \sum_{i=0}^{n-1} \ln \langle e^{-(U(\lambda i+1) - U(\lambda i))/kT} \rangle_{\lambda i} \qquad (5)$$

In eq 5, $U(\lambda_i)$ and $U(\lambda_{i+1})$ are the potential energy functions for the states λ_i and λ_{i+1}, respectively, and $\langle \rangle_{\lambda i}$ refers to an average over the ensemble of configurations generated using $U(\lambda_i)$. Another equivalent expression for ΔA can be employed in free energy difference calculations. It is referred to as the thermodynamic integration (TI) method,[25,27] where ΔA is obtained by eq 6

$$\Delta A = \int_0^1 d\lambda \left\langle \frac{\partial U(\lambda)}{\partial \lambda} \right\rangle_\lambda \qquad (6)$$

A third method, the finite difference thermodynamic integration (FDTI) method,[29] combines the formalisms of PM and TI. FDTI computes numerically the derivatives of the free energy relative to the coupling parameter at fixed values of λ, followed by numerical integration using a quadrature scheme (eq 7). In contrast to PM, the number of λ values to be used in the free energy calculation is not dependent on the degree of overlap between the initial and final phase spaces.

$$\Delta A = -kT \sum_{i=1}^{n} \frac{\ln \langle e^{-[U(\lambda i+\delta\lambda) - U(\lambda i)]/kT} \rangle_i}{\delta\lambda} \qquad (7)$$

In eq 7, n is the number of quadrature points, $\Delta \lambda i$ is a parameter that depends on the numerical integration scheme, and $\delta\lambda$ is the increment used to compute the numerical derivatives. We have recently shown[30,31] that the orthogonality problem that occurs in free energy calculations is adequately treated using the FDTI method. We have also demonstrated that problems of singularity and convergence in free energy calculations can be properly solved by the FDTI method, which uses the Gaussian-Legendre quadrature method for numerical integration, associated with the introduction of a physical criterion to determine the breaking point of a bond or angle described by a harmonic potential. Thus, in this work, we used the FDTI method and employed the same correction procedures as described in refs 30, 31 to calculate free energy differences.

Computational Details

All calculations were performed using a molecular modeling software from MSI , running on a Silicon Graphics O2 R10000 workstation. The *Insight II* program (version 97.0) was employed as a graphical interface for the construction and visualization of molecular structures. The all-atom CVFF force field,[32] within the Discover program (version 2.9.7), was employed in energy minimization and MD simulations. Bond stretching was expressed by a simple harmonic function and the cross terms of the force field were not included in the energy expression. The charges of the noncovalent complexes, including the charges of the inhibitors, were taken from the

CVFF force field. In the covalent complexes, the charges on the Ser195 oxygen and the attacked carbonyl group of APPA and POPBz were taken from the CHARMM force field[33] and adjusted to our system.

First, we obtained from the Brookhaven Protein Data Bank the X-ray crystal structure of the APPA·thrombin·hirugen ternary covalent complex with crystal water molecules (structure 1AHT).[13] The hirugen molecule is bonded to the fibrinogen recognition exosite. In our model, basic residues such as Arg and Lys are protonated, and acid residues such as Asp and Glu are deprotonated. Due to its normal pK_a, the His residues were assumed to be neutral at physiological pH, except for the positively charged His57 in the covalent complex. Keeping the crystal coordinates fixed, only the hydrogen atoms added to the crystal structure were energy minimized. Here, we employed 2000 steps of the steepest descent algorithm followed by 5000 steps of the conjugate-gradient algorithm. Following this procedure, the maximum derivative was less than 0.01 kcal·mol^{-1}·Å^{-1}. To alleviate bad van der Waals contacts, we then fully optimized the entire system. In this step, we employed 5000 steps of the steepest descent algorithm followed by 10000 steps of the conjugate-gradient algorithm leading to a maximum derivative of less than 0.01 kcal·mol^{-1}·Å^{-1}. To obtain $\Delta\Delta A_{reaction}$ for POPBz and APPA, it was necessary to generate a noncovalent complex model from our covalent complex model (see eq 4). To do that, we restored the catalytic triad by disrupting the covalent bond between APPA and Ser195, and transferred the proton from His57 to Ser195. The generated structure was energy minimized, and following this process, a maximum derivative of less than 0.01 kcal·mol^{-1}·Å^{-1} was found.

Then, the hirugen molecule and all residues and water molecules 16 Å away from the C1 atom of APPA (Figure 1) in both covalent and noncovalent complex models were removed. This simplification reduced the number of amino acids to 123. Acetyl and *N*-methylamine blocking groups were used to cap the truncation points. Since we included in our model all the residues with atoms within a radius of 16 Å, our complex model has a radius of approximately 19 Å. Therefore, a 19 Å cap of water molecules was added, centered at the C1 atom of APPA (305 water molecules).

While APPA is neutral at physiological pH, POPBz has a net charge of +1. Thus, in the APPA→POPBz transformation, a positive charge is generated, both in the covalent and noncovalent complexes. The overall charges of both complex models are the same as those of each ligand. In this case, there is no need to include Born term contributions to $\Delta\Delta A_{reaction}$, as both systems have the same radius, the same net charge, and the same dieletric constant outside the finite system.[34,35] To calculate $\Delta\Delta A_{bind(ncov)}$ for APPA and POPBz, it is necessary to compute $\Delta A tr_{(comp(ncov))}$(APPA→POPBz) and $\Delta A tr_{(sol)}$(APPA→POPBz) (see eq 3). As the aqueous phase is neutral, a positive charge is also generated for the APPA→POPBz transformation in solution. Therefore, to minimize Born term contributions to $\Delta\Delta A_{bind(ncov)}$ in this case, the aqueous phase was obtained by surrounding APPA with a water sphere of 19 Å, centered at the C1 atom of APPA (see Figure 1), including a total of 944 water molecules. To obtain $\Delta\Delta A_{hyd}$ for APPA and POPBz, we need to compute $\Delta A tr_{(sol)}$(APPA→POPBz) and $\Delta A tr_{(g)}$(APPA→POPBz). As conventional periodic boundary conditions are not appropriate to solvate a solute when the charge varies in the transformation,[36,37] we solvated APPA using the same spherical 19 Å cap of water described above. As one of the transformations is performed in the gas phase, a Born term contribution of -8.63 kcal/mol had to be added to $\Delta\Delta A_{hyd}$.

Except for the APPA→POPBz transformation, there was no charge variation in the remaining mutations (see Figures 1 and 2). This eliminated the need for including Born term contributions. Thus, to obtain $\Delta\Delta A_{hyd}$ for these cases, POPBz was centered in a 20 Å cubic box (~250 water molecules) using periodic boundary conditions (PBC), and then the sucessive transformations POPBz→PPBz, PPBz→PEBz, PEBz→PMBz and PMBz→Bz were performed. To calculate the relative free

energy of binding for these transformations ($\Delta\Delta A_{bind(ncov)}$), it was necessary to calculate $\Delta A tr_{(comp(ncov))}(X \rightarrow Y)$ and $\Delta A tr_{(sol)}$-$(X \rightarrow Y)$. The initial system for these transformations inside the solvated noncovalent complex model was obtained from the last configuration of the APPA→POPBz transformation. As shown by Essex and Jorgensen,[38] the use of a spherical cap of water rather than the conventional periodic boundary conditions affects the calculated free energies of hydration in simple systems. Therefore, to cancel the errors introduced by the application of a spherical cap of water in the solvated noncovalent complex model, we employed an identical approximation for the calculation of $\Delta A tr_{(sol)}(X \rightarrow Y)$. The initial system for transformations in the aqueous phase was obtained from the last configuration of the APPA→POPBz transformation in solution.

Initial preparation of all preliminary systems (covalent and noncovalent complexes APPA·thrombin, APPA in solution ($R = 19$ Å) and POPBz in solution (PBC)) consisted of an energy minimization calculation (2000 steps of the steepest descent algorithm followed by 5000 steps of the conjugate-gradient algorithm), followed by 20 ps of an MD run, to which we applied the *NVT* ensemble. We kept the solute atoms fixed throughout the entire preparation process. This step was performed in order to relax water molecules in the aqueous phase and in the solvated complex models to the solute potential. Then, all coordinates of the systems were fully optimized. Because of the absence of discarded residues, the methyl carbon atom of acetyl and *N*-methylamine blocking groups in the solvated complex model were kept fixed to avoid any anomalous behavior in the protein structure. At this point, we employed 5000 steps of the steepest descent algorithm followed by 10000 steps of the conjugate-gradient algorithm. At the end of this procedure, the maximum derivative was less than 0.01 kcal.mol^{-1}Å^{-1}.

Next, we performed the sucessive transformation simulations. Each transformation, regardless of the environment, was achieved by an MD run of 1.2 ns using the FDTI method to compute free energy differences. The initial and final states were linearly coupled through the λ parameter. The number of quadrature points, n, used in the calculations was six. The values of $\Delta\lambda i$ ($\Delta\lambda 1 = 0.0857$, $\Delta\lambda 2 = 0.1804$, $\Delta\lambda 3 = 0.2340$, $\Delta\lambda 4 = 0.2340$, $\Delta\lambda 5 = 0.1804$, $\Delta\lambda 6 = 0.0857$) and the quadrature points ($\lambda 1 = 0.03377$, $\lambda 2 = 0.16940$, $\lambda 3 = 0.38069$, $\lambda 4 = 0.61931$, $\lambda 5 = 0.83060$, $\lambda 6 = 0.96623$) (see eq 7) were automatically calculated by the Gaussian-Legendre quadrature method.[39] The increment $\delta\lambda$ used in eq 7 was 0.0005.

All transformations were performed using MD simulations in an *NVT* ensemble ($T = 300$ K), employing the single topology approach by mixing the force field parameters (force constants, equilibrium bond lengths, charges, etc.). In the APPA→POPBz transformation, the carboxylate group of APPA was mutated into the methyl group of POPBz. To keep the number of atoms fixed, the carboxylate oxygens and a dummy atom (Du) were transformed into the three hydrogen atoms of the methyl group. In the POPBz→PPBz transformation, the carbonyl group of POPBz was mutated into the methylene group of PPBz. In this case, to keep the number of atoms fixed, the carbonyl oxygen and a dummy atom were transformed into the hydrogen atoms of the methylene group. All other simulations involved the mutation of a methyl group into a hydrogen atom. Therefore, the hydrogen atoms of the methyl groups were also substituted by dummy atoms. The C−Du and H−Du equilibrium bond lengths were not shrunk, and all energy terms (including bonded terms of the force field) of the dummy atoms were turned off in the simulations.

The equations of motion were integrated every 1.0 fs using the Verlet Leapfrog algorithm.[40] All bonds and angles were allowed to move in the simulations. In all simulations, the ensemble average of the Boltzmann factor, $e^{-\Delta U/kT}$, was evaluated through a MD run of 100 ps after a 100 ps of equilibration at each λi, giving a total of 1.2 ns of simulation for each transformation. For further analysis, the trajectory was sampled every 1.0 ps. The convergence at each λi was verified by plotting the Boltzmann factor vs time. The FDTI method

computes $\Delta A i/\delta\lambda$ at each λi sampling both forward ($\Delta A(\lambda i \rightarrow \lambda i + \delta\lambda)/\delta\lambda$) and backward ($\Delta A(\lambda i \rightarrow \lambda i - \delta\lambda)/\delta\lambda$). $\Delta A i/\delta\lambda$ at λi is the first quantity plus the negative of the second one, divided by two. Similar values for ($\Delta A(\lambda i \rightarrow \lambda i + \delta\lambda)/\delta\lambda$) and ($-\Delta A(\lambda i \rightarrow \lambda i - \delta\lambda)/\delta\lambda$) are an additional measure of convergence.

During MD runs, the temperature was maintained at 300 K via the velocity-scaling algorithm[41] at the equilibration stage, and via a weak coupling to an external temperature bath with a time constant of 0.1 ps[42] at the data collection stage. To prevent the evaporation of water molecules, a half-harmonic restraining potential of 0.5 kcal·mol^{-1}·Å^{-2} was used when the distance between a water oxygen atom and the center of the solvation model exceeded 19 Å. For reasons mentioned above, the methyl carbon atoms of the blocking groups were kept fixed in the MD transformation simulations occurring inside the solvated complex models.

To save computational time, a spherical residue-based nonbonded interaction cutoff of 10 Å was applied to all transformations, except for APPA→POPBz. To "turn off" the interactions smoothly, we employed a quintic spline function from 8.5 to 10 Å. In this manner, discontinuities in the potential energy surface were minimized. Whenever an atom moved more than half the length of the buffer region (between 10 and 11 Å), the neighbor list was updated. This ensured that no atoms outside the buffer region were able to move close enough to interact. Since a positive charge is generated in the APPA→POPBz transformation, the Born term correction is only valid if all atoms inside the sphere of 19 Å interact with each other. In this case, we applied the double-cutoff methodology.[43] The first cutoff has 10 Å of radius, while the radius of the second cutoff is long enough to include interactions of all atoms with every other atom.

Results and Discussion

Analysis of the Hydration Order. Table 1 gives calculated values of the single and double free energy differences for the transformations performed in this work. As discussed in ref 30, we could not determine precisely the relative free energy of hydration for PMBz and Bz. Still, we pointed out that $\Delta\Delta A_{hyd}$ between these compunds should lie somewhere between 1.47 and 3.84 kcal/mol. Jorgensen and Nguyen showed that the penalty for creating a larger cavity in transforming an aromatic hydrogen into a methyl group in substituted benzenes is matched by the enhanced VDW interactions between the latter and water.[44] Thus, the difference of hydration between PMBz and Bz is probably derived from other contributions. Since the classical dipole moments for Bz and PMBz calculated from the CVFF partial charges with respect to coordinate axes centered on each molecule's center of mass are 6.94 and 12.18 D, respectively,[30,31] PMBz should be more solvated than Bz because of stronger electrostatic interactions with the water molecules.

On the other hand, differing from the relative hydration between PMBz and Bz, the analysis of $\Delta\Delta A_{hyd}$ suggests that for PPBz→PEBz and PEBz→PMBz the penalty for creating a larger cavity, while mutating an hydrogen atom into a methyl group, is greater than the enhanced VDW interactions between the latter and water. In transforming PMBz in Bz, the methyl group is partially shielded from the solvent and the cavity term is less important. However, as the carbon chains of PEBz and PPBz are more exposed to the solvent, especially in PPBz, the cavity term becomes more significant than the VDW interactions when one annihilates a methyl group in PPBz→PEBz and PEBz→PMBz. Consequently, while PMBz is better

Table 1. Free-Energy Changes Calculated by the FDTI Method (kcal/mol)[a]

transformation	APPA→POPBz	POPBz→PPBz	PPBz→PEBz	PEBz→PMBz	PMBz→Bz
$\Delta A\mathrm{tr}_{(g)}$	-19.20 ± 0.31	38.61 ± 0.22	9.93 ± 0.20	-21.77 ± 0.25	-10.51 ± 0.10 -8.56 ± 0.08^{b}
$\Delta A\mathrm{tr}_{(sol)}$ (PBC)	n.c.	41.96 ± 0.31	-11.39 ± 0.32	-22.88 ± 0.28	-9.04 ± 0.35 -4.72 ± 0.27^{b}
$\Delta A\mathrm{tr}_{(sol)}$ (19 Å)	16.45 ± 0.98	42.80 ± 0.22	-11.29 ± 0.30	-24.07 ± 0.30	-5.73 ± 0.28
$\Delta A\mathrm{tr}_{(comp(ncov))}$	-41.19 ± 1.58	44.84 ± 0.22	-11.88 ± 0.30	-21.79 ± 0.31	-5.08 ± 0.26
$\Delta A\mathrm{tr}_{(comp(cov))}$	-36.74 ± 1.67	-	-	-	-
$\Delta\Delta A_{hyd}$	35.65 ± 1.29 $(27.02 \pm 1.29)^{c}$	3.35 ± 0.53	-1.46 ± 0.52	-1.11 ± 0.53	1.47 ± 0.45 3.84 ± 0.35
$\Delta\Delta A_{bind(ncov)}$	-57.64 ± 2.56	2.04 ± 0.44	-0.59 ± 0.60	2.29 ± 0.61	0.65 ± 0.54
$\Delta\Delta A_{reaction}$	4.45 ± 3.25	-	-	-	-
$\Delta\Delta A_{bind(cov)}$	-53.19 ± 2.65	-	-	-	-
$\Delta\Delta A_{bind}\mathrm{exp}^{d}$	n.a.	n.a.	n.a.	n.a.	0.68

n.c., not calculated; n.a., not available. [a] The FDTI method was employed to compute the potential energy contribution to the Helmholtz free energy (see text). The reported errors are the standard deviation of the Boltzmann factor obtained during the data collection stage of the simulation. (g), free energy computed in the gas phase; (PBC), in the aqueous phase using periodic boundary conditions; (19 Å), in the aqueous phase using a spherical cap of water with 19 Å of radius, (comp(ncov)) and (comp(cov)) inside the solvated noncovalent and covalent complex models, respectively, using a spherical cap of water with 19 Å of radius. [b] As discussed in ref 30, we could not determine precisely the relative free energy of hydration for PMBz and Bz. $\Delta\Delta A_{hyd}$ between these compounds lies somewhere between 1.47 and 3.84 kcal/mol. [c] The value of $\Delta\Delta A_{hyd}$ in parentheses includes a Born term contribution of -8.63 kcal/mol. [d] Reference 30.

solvated than PEBz by 1.11 kcal/mol, PEBz is better solvated than PPBz by 1.46 kcal/mol.

The calculated $\Delta\Delta A_{hyd}$ shows that POPBz is more solvated than PPBz by 3.35 kcal/mol. The results also show that POPBz is more solvated than PEBz, PMBz, and Bz. This was expected since the carbonyl group of POPBz is hydrogen bonded to the water molecules of the solvent. However, because of its zwitterion form in solution, APPA is the best solvated compound of the series. As $\Delta\Delta A_{hyd}$ for PMBz and Bz lies between 1.47 and 3.84 kcal/mol, it is not possible to determine if the least solvated compound of the series is Bz or PPBz. Consequently, analysis of the relative hydration reveals two possible hydration orders for the para-substituted benzamidine derivatives: APPA > POPBz > PMBz > PEBz > PPBz > Bz and APPA > POPBz > PMBz > PEBz > Bz > PPBz.

Analysis of the Binding Order. The binding process between APPA and thrombin involves two major steps. The first is the formation of a noncovalent enzyme·APPA complex (the Michaelis complex). The second is the formation of a covalent bond between APPA and thrombin. As protein crystallography reflects relatively stable and long-lived structures,[45] and as the X-ray crystal structure of the APPA·thrombin complex shows a tetrahedral intermediate between them,[13] the covalent complex in this case should be more stable thermodynamically than the noncovalent complex. Therefore, the inhibition constant of thrombin by APPA must represent the complete thermodynamic process, with APPA and thrombin unbound in solution as the initial state and the tetrahedral intermediate as the final state. Electrophilic compounds and noncovalent compounds interact with the enzyme via different mechanisms. While the first interacts covalently with thrombin, the second interacts noncovalently. This makes calculation of the relative free energy of binding to thrombin by the FEP method between these two classes of molecules unfeasible. Therefore, connection between the two classes was accomplished by using the experimental binding constants for APPA (K_i = 620 nM)[11,13] and Bz (K_i = 300 nM).[14,15]

In the APPA→POPBz transformation, with the exception of simulations in the gas and aqueous phases,

we observed very poor convergence of the Boltzmann factor, shown in eq 7 ($e^{-[U(\lambda i+\delta\lambda) - U(\lambda i)]/kT}$). However, it is not clear if the poor convergence is a consequence of the application of the double cutoff methodology to the generation of a positive charge inside the protein, or if it is derived from short MD simulations. What seems clear is that it affects $\Delta A\mathrm{tr}_{(comp(ncov))}$ and $\Delta A\mathrm{tr}_{(comp(cov))}$, and consequently $\Delta\Delta A_{bind(ncov)}$ and $\Delta\Delta A_{reaction}$ for the APPA→POPBz transformation. Nevertheless, this is probably more important to $\Delta\Delta A_{bind(ncov)}$ than to $\Delta\Delta A_{reaction}$ as the errors in the quantities $\Delta A\mathrm{tr}_{(comp(ncov))}$ and $\Delta A\mathrm{tr}_{(comp(cov))}$ tend to cancel each other. As a result, the reaction between APPA and thrombin is 4.45 kcal/mol more favorable thermodynamically than the reaction between POPBz and the enzyme (Table 1). On the other hand, it is reasonable to assume that the simulation protocol is appropriate for the simulations without charge variation because of a small hysteresis obtained in our recently reported results for the PMBz→Bz transformation in both directions.[30] The results shown in Table 1 for the PMBz→Bz transformation ($\Delta A\mathrm{tr}_{(sol)}$ (19 Å), $\Delta A\mathrm{tr}_{(comp(ncov))}$, and $\Delta\Delta A_{bind(ncov)}$) are then an average of both directions.

Table 1 shows that for the APPA→POPBz transformation $\Delta\Delta A_{bind(ncov)}$ and, consequently, $\Delta\Delta A_{bind(cov)}$ are too negative, since APPA is an active thrombin inhibitor. However, although $\Delta\Delta A_{bind(ncov)}$ is not accurate in this case, the K_i values for APPA[11,13] and Bz,[14,15] which give a experimental $\Delta\Delta A_{bind}$ of -0.43 kcal/mol at 300 K between these two compounds, and the values of $\Delta\Delta A_{bind(ncov)}$ for the other transformations (Table 1), taken together, indicate that the noncovalent association Bz.thrombin is only more favorable than the covalent association APPA.thrombin. Since the covalent APPA·thrombin complex is more stable than the noncovalent APPA·thrombin complex, as discussed above, APPA may be pointed as the worst ligand in the series to bind noncovalently to thrombin, probably because (i) APPA is the most solvated ligand of the series, and (ii) there is a number of electrostatic repulsions between the carboxylate group of APPA and negative residues in the active site of the noncovalent complex (Glu192, Asp102, and Aps189, see below).
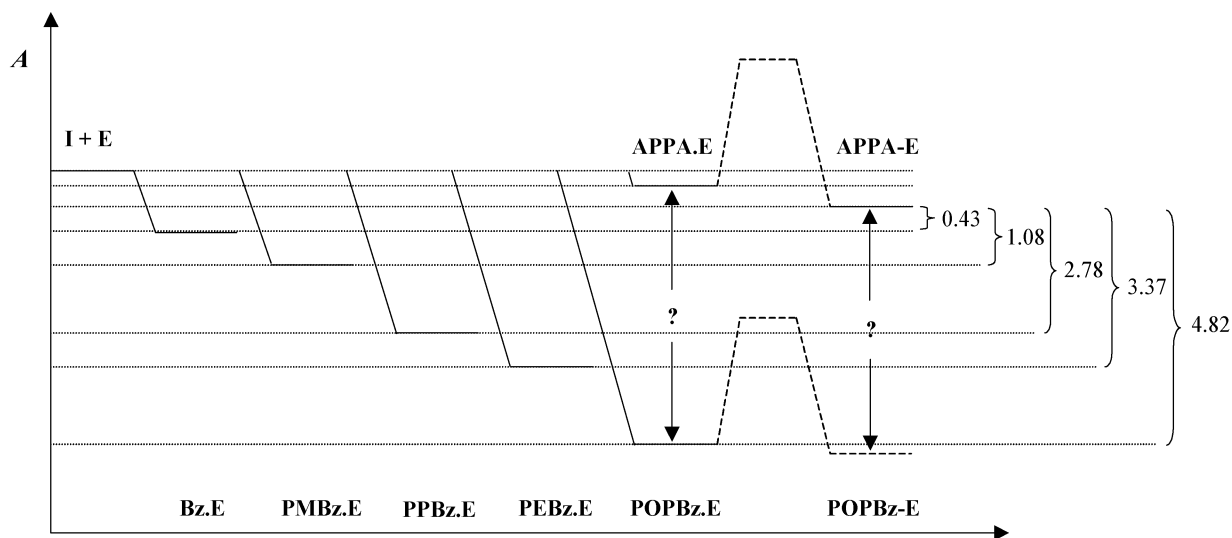
Figure 3. Schematic representation of the relative free energies of binding to thrombin for all compounds with respect to APPA.

Although Bz, as mentioned above, is the least solvated (or the second least solvated) compound, it only binds to thrombin better than APPA. This suggests that, despite a small desolvation penalty, the weak interaction with the enzyme makes the association Bz·thrombin less favorable than the association between the enzyme and PMBz, PPBz, PEBz, and POPBz. Analysis of $\Delta\Delta A_{hyd}$ and $\Delta\Delta A_{bind(ncov)}$ for PEBz→PMBz shows that although PMBz is better solvated than PEBz, the association PMBz·thrombin is less favorable than the association PEBz·thrombin because of weaker interactions between PMBz and the enzyme. On the other hand, analysis of $\Delta\Delta A_{hyd}$ and $\Delta\Delta A_{bind(ncov)}$ for PPBz→PEBz shows that the higher desolvation penalty of PEBz is overcome by a stronger noncovalent interaction between this compound and the enzyme when compared to PPBz. Finally, although POPBz is the second most solvated compound, $\Delta\Delta A_{bind(ncov)}$ points out that it is the best ligand in the series to bind noncovalently to thrombin. This suggests that the desolvation penalty of POPBz is overcome by a strong noncovalent interaction between this compound and the enzyme. Thus, the compounds bind thrombin noncovalently in the following order: POPBz > PEBz > PPBz > PMBz > Bz > APPA.

Assuming that POPBz is a typical electrophilic inhibitor, it should have an even greater affinity for the enzyme than the other benzamidine derivatives when the covalent complex between POPBz and thrombin is formed. However, it is difficult to determine this greater affinity with accuracy since $\Delta\Delta A_{bind(cov)}$ between APPA and POPBz is too negative. On the other hand, the experimental K_i values for APPA and Bz indicate that even if the formation of the covalent complex with thrombin occurs, APPA remains the worst ligand to bind to the enzyme. As mentioned above, the connection between the electrophilic compounds and the noncovalent compounds was accomplished by the experimental binding constants for APPA and Bz, and the calculation of the relative free energies of noncovalent binding. This gives a final binding order, including the reaction step, of POPBz > PEBz > PPBz > PMBz > Bz > APPA. More specifically, Bz, PMBz, PPBz, PEBz, and POPBz bind to thrombin better than APPA by 0.43 kcal/mol, 1.08

kcal/mol, 2.78 kcal/mol, 3.37 kcal/mol, and <53.19 kcal/mol, respectively. If POPBz is not an electrophilic inhibitor, it will bind to thrombin better than APPA by 4.82 kcal/mol. Therefore, POPBz would still be the best candidate of the series. The quality of our results is supported by very good agreement between the experimental[30] and the calculated $\Delta\Delta A_{bind}$ between PMBz and Bz (Table 1). Figure 3 shows schematically the relative free energies of binding to thrombin for all studied compounds with respect to APPA. It is interesting to note that all candidates proposed in this work have a higher affinity for the enzyme than the compounds selected from the literature, APPA and Bz.

Analysis of Interactions with the Enzyme. The addition of $\Delta\Delta A_{bind(ncov)}$ to $\Delta\Delta A_{hyd}$ eliminates the desolvation step and restricts our analysis to ligand-enzyme noncovalent interactions. Our calculations show that the noncovalent interaction between POPBz and thrombin is more favorable than PEBz, PMBz, PPBz, Bz, and APPA by 3.34 kcal/mol, 4.52 kcal/mol, 5.39 kcal/mol, 6.64 to 9.01 kcal/mol, and < 30.62 kcal/mol, respectively. The high similarity between the order of noncovalent interactions with the enzyme and the order of noncovalent binding suggests that noncovalent interactions with the enzyme are more important than the desolvation penalty during formation of the Michaelis complex.

Figures 4A−F show the noncovalent interactions between each compound and thrombin. They demonstrate that the amidino group in all compounds is hydrogen bonded to the carbonyl oxygen of Gly219 and form a water-mediated salt bridge with Asp189. Figure 4A suggests that POPBz interacts more strongly with thrombin because of the additional hydrogen bond between its carbonyl group and the N−H group of Gly193. Inspection of Figures 4B, 4C, and 4D suggests that the ethyl group in the para position of the aromatic ring fits well in the hydrophobic cavity formed by His57, Ala190, Glu192, Gly193, and Val213 and that the methyl group of PMBz and the propyl group of PPBz are either too small or too big. Figure 4E illustrates the fact that the lack of interaction between a hydrophobic substituent in the para position of the ring and the hydrophobic cavity worsens the binding of Bz to throm-
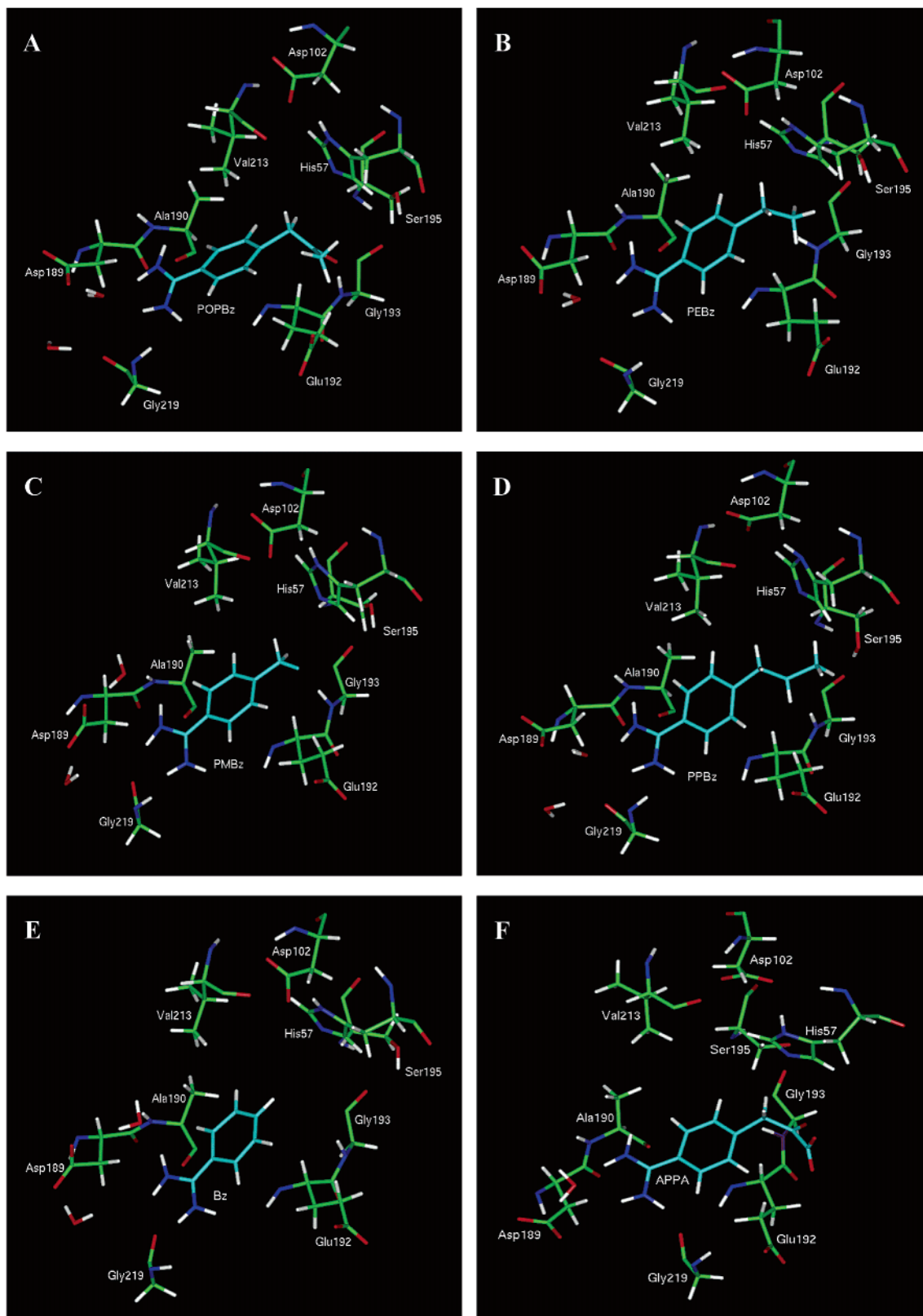
Figure 4. A. The last configuration of the APPA→POPBz transformation at $\lambda 6$ (the hybrid group is ~97% of a methyl group). B. The last configuration of the PPBz→PEBz transformation at $\lambda 6$ (the hybrid group is ~97% of a hydrogen atom). C. The last configuration of the PEBz→PMBz transformation at $\lambda 6$ (the hybrid group is ~97% of a hydrogen atom). D. The last configuration of the POPBz→PPBz transformation at $\lambda 6$ (the hybrid group is ~97% of a methylene group). E. The last configuration of the PMBz→Bz transformation at $\lambda 6$ (the hybrid group is ~97% of a hydrogen atom). F. The last configuration of the APPA→POPBz transformation at $\lambda 1$ (the hybrid group is ~97% of a carboxylate group). All transformations performed inside the solvated noncovalent complex model.

bin. Finally, Figure 4F indicates that the noncovalent interaction of APPA to thrombin is the poorest of the

series due to a number of electrostatic repulsions between the carboxylate group of APPA and negative
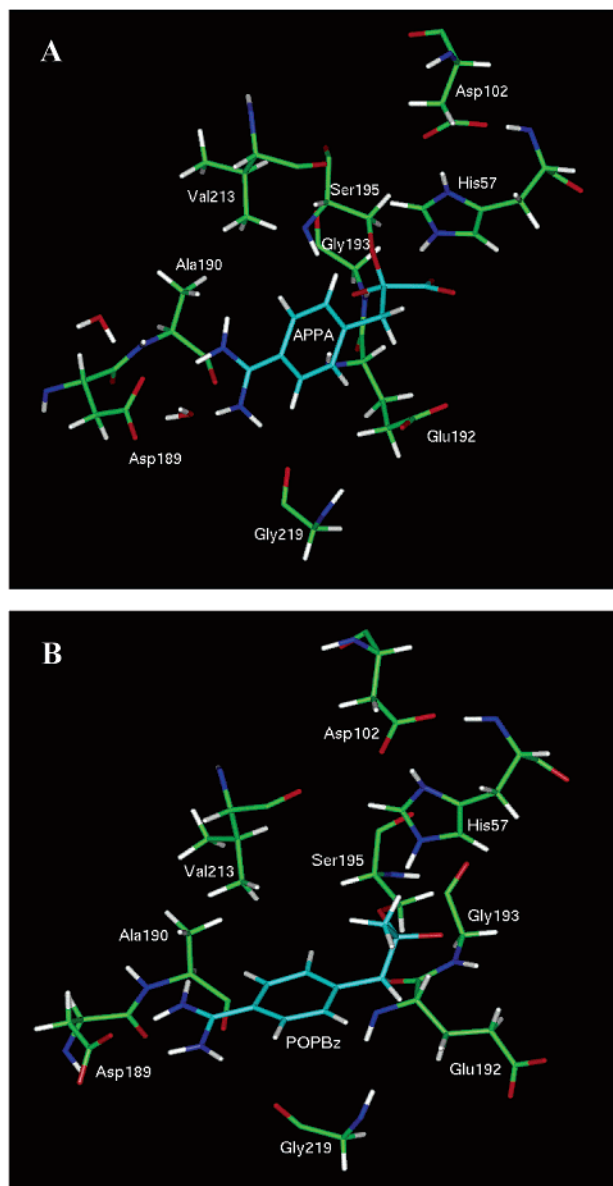
Figure 5. A. The last configuration of the APPA→POPBz transformation at $\lambda 1$ (the hybrid group is ~97% of a carboxylate group). B. The last configuration of the APPA→POPBz transformation at $\lambda 6$ (the hybrid group is ~97% of a methyl group). APPA→POPBz transformation performed inside the solvated covalent complex model.

residues in the active site (Glu192, Asp102, and Aps189). Moreover, as a result of electrostatic repulsion between the carboxylate group of APPA and Glu192, the additional hydrogen bond between the carbonyl group of APPA and the N—H group of Gly193 (observed for POPBz) cannot be formed.

Figures 5A and 5B show the tetrahedral intermediate structures formed after proton transfer from Ser195 to His57, which is concerted to the nucleophilic attack to the carbonyl groups of APPA and POPBz, supposing POPBz is an electrophilic inhibitor. They suggest that the reaction between thrombin and APPA is more favorable thermodynamically than the reaction between POPBz and the enzyme ($\Delta\Delta A_{reaction}$ = 4.45 kcal/mol) due to a strong electrostatic attraction between the positive charge of the protonated His57 and the negative charge of the carboxylate group of APPA. In any event, as

covalent binding includes the noncovalent binding and reaction steps, POPBz binds much more strongly to thrombin than APPA.

The addition of $\Delta\Delta A_{bind}$ to $\Delta\Delta A_{hyd}$ eliminates the desolvation step and restricts our analysis to ligand–enzyme interactions (noncovalent for noncovalent compounds, and covalent and noncovalent for electrophilic compounds). If POPBz is not an electrophilic inhibitor, the interaction between APPA and thrombin will be stronger than the noncovalent interaction between thrombin and POPBz, PEBz, PMBz, PPBz, and Bz by 22.20 kcal/mol, 25.54 kcal/mol, 26.72 kcal/mol, 27.59 kcal/mol, and 28.84 to 31.21 kcal/mol, respectively. This is probably due to the formation of a covalent bond between the hydroxyl oxygen of Ser195 and the carbonyl carbon of APPA, and to the electrostatic attraction between the positive charge of His57, which is protonated in the tetrahedral intermediate, and the negative charge of the carboxylate group of APPA. Accordingly, the order of interaction with the enzyme is APPA > POPBz > PEBz > PMBz > PPBz > Bz. On the other hand, if POPBz is an electrophilic inhibitor, the interaction between APPA and thrombin will be <26.17 kcal/mol weaker than the interaction between POPBz and thrombin. In this case, both APPA and POPBz are covalently bonded to thrombin, and this difference would be a consequence of the absence of electrostatic repulsions between the carboxylate group of APPA and negative residues in the active site for POPBz, even though the electrostatic attraction between the protonated His57 and the carboxylate group of APPA is missing in the POPBz–thrombin complex. Accordingly, the order of interaction with the enzyme is POPBz > APPA > PEBz > PMBz > PPBz > Bz. Comparison of the two possible orders of interaction with the calculated binding order, POPBz > PEBz > PPBz > PMBz > Bz > APPA, makes it clear that APPA has the lowest affinity for the enzyme due to a great desolvation penalty.

Conclusions

In this work, we showed that hydrogen bonds with the N—H group of Gly193 and hydrophobic interactions with the wall of the cavity formed by His57, Ala190, Glu192, Gly193, and Val213 increase the binding affinity for thrombin. Moreover, we showed that it is wise to avoid the design of candidates with a negatively charged group because of electrostatic repulsions with negative residues in the active site, and because of a large desolvation penalty. It is also interesting to note that the addition of more lipophilic groups and the elimination of negatively charged groups would improve the pharmacokinetic profile of the thrombin inhibitor candidates by increasing their intestinal permeability. To conclude, the calculated binding order, including or not the reaction step between POPBz and the enzyme, POPBz > PEBz > PPBz > PMBz > Bz > APPA, shows that all candidates proposed in this work have a higher affinity for the enzyme than APPA and Bz, compounds originally selected from the literature.

References

(1) Coburn, C. A.; Rush, D. M.; Williams, P. D.; Homnick, C.; Lyle, E. A.; Lewis, S. D.; Lucas, B. J., Jr.; Di Muzio-Mower, J. M.; Juliano, M.; Krueger, J. A.; Vastag, K.; Chen, I.-W.; Vacca, J. P. Bicyclic Pyridones as Potent, Efficacious and Orally Bioavailable Thrombin Inhibitors. *Bioorg. Med. Chem. Lett.* **2000**, *10*, 1069−1072.

(2) Pavone, V.; De Simone, G.; Nastri, F.; Galdiero, S.; Staiano, N.; Lombardi, A.; Pedone, C. Multiple Binding Mode of Reversible Synthetic Thrombin Inhibitors. A Comparative Structural Analysis. *J. Biol. Chem.* **1998**, *379*, 987−1006.

(3) Lee, K. Recent Progress in Small Molecule Thrombin Inhibitors. *Korean J. Med. Chem.* **1997**, *7* (2), 127−144.

(4) Kimbal, S. D. Thrombin Active Site Inhibitors. *Curr. Pharm. Des.* **1995**, *1*, 441−468.

(5) Ripka, W. C. New Thrombin Inhibitors in Cardiovascular Disease. *Curr. Opin. Chem. Biol.* **1997**, *1*, 242−253.

(6) Wienand, A.; Ehrhardt, C.; Metternich, R.; Tapparelli, C. Design, Synthesis and Biological Evaluation of Selective Boron-Containing Thrombin Inhibitors. *Bioorg. Med. Chem. Lett.* **1999**, *7*, 11295−1307.

(7) Lu, T.; Soll, R. M.; Illig, C. R.; Bone, R.; Murphy, L.; Spurlino, J.; Salemme, F. R.; Tomczuk, B. E. Structure−Activity and Crystallographic Analysis of a New Class of Non-Amide-Based Thrombin Inhibitor. *Bioorg. Med. Chem. Lett.* **2000**, *10*, 79−82.

(8) Lu, T.; Tomczuk, B.; Bone, R.; Murphy, L.; Salemme, F. R.; Soll, R. M. Non-Peptidic Phenyl-Based Thrombin Inhibitors: Exploring Structural Requirements of the S1 Specificity Pocket with Amidines. *Bioog. Med. Chem. Lett.* **2000**, *10*, 83−85.

(9) Lee, K.; Jung, W.-H.; Kang, M.; Lee, S.-H. Noncovalent Thrombin Inhibitors Incorporating an Imidazolylethynyl P1. *Bioorg. Med. Chem. Lett.* **2000**, *10*, 2775−2778.

(10) Lumma, W. C., Jr.; Witherup, K. M.; Tucker, T. J.; Brady, S. F.; Sisko, J. T.; Naylor-Olsen, A. M.; Lewis, S. D.; Lucas, B. J.; Vacca, J. P. Design of Novel, Potent, Noncovalent Inhibitors of Thrombin with Nonbasic P-1 Substructures: Rapid Structure−Activity Studies by Solid-Phase Synthesis. *J. Med. Chem.* **1998**, *41*, 1011−1013.

(11) Babine, R. E.; Bender, S. L. Molecular Recognition of Protein−Ligand Complexes: Applications to Drug Design. *Chem. Rev.* **1997**, *97* (5), 1359−1472.

(12) Jones-Hertzog, D. K.; Jorgensen, W. L. Binding Affinities for Sulfonamide Inhibitors with Human Thrombin Using Monte Carlo Simulations with a Linear Response Methodology. *J. Med. Chem.* **1997**, *40*, 1539−1549.

(13) Chen, Z.; Li, Y.; Mulichak, A. M.; Lewis, S. D.; Shafer, J. A. Crystal Structure of Human α-Thrombin Complexed with Hirugen and p-Amidinophenylpyruvate at 1.6 Å Resolution. *Arch. Biochem. Biophys.* **1995**, *322* (1), 198−203.

(14) Banner, D.; Hadváry, P. Crystallographic Analysis at 3.0-Å Resolution of the Binding to Human Thrombin of Four Active Site-Directed Inhibitors. *J. Biol. Chem.* **1991**, *266* (30), 20085−20093.

(15) Scozzafava, A.; Briganti, F.; Supuran, C. T. Protease Inhibitors − Part 3. Synthesis of Non-Basic Thrombin Inhibitors Incorporating Pyridinium-Sulfanilylguanidine Moieties at the P1 Site. *Eur. J. Med. Chem.* **1999**, *34*, 939−952.

(16) Tucker, T. J.; Brady, S. F.; Lumma, W. C.; Lewis, S. D.; Gardell, S. J.; Naylor-Olsen, A. M.; Yan, Y.; Sisko, J. T.; Stauffer, K. J.; Lucas, B. J.; Lynch, J. J.; Cook, J. J.; Stranieri, M. T.; Holahan, M. A.; Lyle, E. A.; Baskin, E. P.; Chen, I.-W.; Dancheck, K. B.; Krueger, J. A.; Cooper, C. M.; Vacca, J. P. Desing and Synthesis of a Series of Potent and Orally Bioavailable Noncovalent Inhibitors That Utilize Nonbasic Groups in the P1 Position. *J. Med. Chem.* **1998**, *41*, 3210−3219.

(17) Bone, R.; Lu, T.; Illig, C. R.; Soll, R. M.; Spurlino, J. C. Structural Analysis of Thrombin Complexed with Potent Inhibitors Incorporating a Phenyl Group as a Peptide Mimetic and Aminopyridines as Guanidine Substitutes. *J. Med. Chem.* **1998**, *41*, 2068−2075.

(18) Lumma, W. C., Jr.; Witherup, K. M.; Tucker, T. J.; Brady, S. F.; Sisko, J. T.; Naylor-Olsen, A. M.; Lewis, S. D.; Lucas, B. J.; Vacca, J. P. Design of Novel, Potent, Noncovalent Inhibitors of Thrombin with Nonbasic P-1 Substructures: Rapid Structure−Activity Studies by Solid-Phase Synthesis. *J. Med. Chem.* **1998**, *41*, 1011−1013.

(19) Isaacs, R. C. A.; Cutrona, K. J.; Newton, C. L.; Sanderson; P. E. J.; Solinsky, M. G.; Baskin, E. P.; Chen, I.-W.; Cooper, C. M.; Cook, J. J.; Gardell, S. J.; Lewis, S. D.; Lucas Jr., R. J.; Lyle, E. A.; Lynch, J. J., Jr.; Naylor-Olsen, A. M.; Stranieri, M. T.; Vastag, K.; Vacca, J. P. C6 Modifications of the Pyridone Core of Thrombin Inhibitor L-374,087 as a Means of Enhancing Its Oral Absorption. *Bioorg. Med. Chem. Lett.* **1998**, *8*, 1719−1724.

(20) Sanderson, P. E. J.; Lyle, T. A.; Cutrona, K. J.; Dyer, D. L.; Dorsey, B. D.; McDonough, C. M.; Naylor-Olsen, A. M.; Chen, I.-W.; Chen, Z.; Cook, J. J.; Cooper, C. M., Gardell, S. J.; Hare, T. R.; Krueger, J. A.; Lewis, S. D.; Lin, J. H.; Lucas, B. J., Jr.; Lyle, E. A.; Lynch, J. J., Jr.; Stranieri, M. T.; Vastag, K.; Yan, Y.; Shafer, J. A.; Vacca, J. P. Efficacious, Orally Bioavailable Thrombin Inhibitors Based on 3-Aminopyridinone or 3-Aminopyrazinone Acetamide Peptidomimetic Templates. *J. Med. Chem.* **1998**, *41*, 4466−4474.

(21) Tucker, T. J.; Lumma, W. C.; Lewis, S. D.; Gardell, S. J.; Lucas, B. J.; Baskin, E. P.; Woltmann, R.; Lynch, J. J.; Lyle, E. A.; Appleby, S. D.; Chen, J. W.; Dancheck, K. B., Vacca, Potent Noncovalent Thrombin Inhibitors that Utilize The Unique Amino Acid D-Dicyclohexylalanine in the P3 Position. Implications on Oral Bioavailability and Antithrombotic Efficacy. J. P. *J. Med. Chem.* **1997**, *40*, 1565−1569.

(22) Lee, K.; Hwang, S. Y.; Park, C. W. Thrombin Inhibitors Based on a Propargylglycine Template. *Bioorg. Med. Chem. Lett.* **1999**, *9*, 1013−1018.

(23) Bachand, B.; Tarazi, M.; St-Denis, Y.; Edmunds, J. J.; Winocour, P. D.; Leblond, L. Siddiqui, M. A. Potent and Selective Bicyclic Lactam Inhibitors of Thrombin. Part 4: Transition State Inhibitors. *Bioorg. Med. Chem. Lett.* **2001**, *11*, 287−290.

(24) Zwanzig, R. High-Temperature Equation of State by a Perturbation Method. I. Nonpolar Gases. *J. Chem. Phys.* **1954**, *22* (8), 1420−1426.

(25) Beveridge, D. L.; DiCapua, F. M. Free Energy via Molecular Simulations. *Annu. Rev. Biophys. Biophys. Biochem.* **1989**, *18*, 431−492.

(26) Jorgensen, W. L. Free Energy Calculations: A Breakthrough for Modeling Organic Chemistry in Solution. *Acc. Chem. Res.* **1989**, *22*, 184−189.

(27) Kollman, P. A. Free Energy Calculations: Applications to Chemical and Biochemical Phenomena. *Chem. Rev.* **1993**, *93*, 2395−2417.

(28) Wong, C. F.; McCammon, A. Dynamics and Design of Enzymes and Inhibitors. *J. Am. Chem. Soc.* **1986**, *108* (13), 3830−3832.

(29) Mezei, M. The Finite Difference Thermodynamic Integration, Tested on Calculating the Hydration Free Energy Difference Between Acetone and Dimethylamine in Water. *J. Chem. Phys.* **1987**, *86* (12), 7084−7088.

(30) Guimarães, C. R. W.; Bicca de Alencastro, R. Thermodynamic Analysis of Thrombin Inhibition by benzamidine and *p*-methylbenzamidine via Free-Energy Perturbations: Inspection of Intraperturbed-Group Contributions Using the Finite Difference Thermodynamic Integration (FDTI) Algorithm. *J. Phys. Chem. B* **2002**, *106* (2), 466−476.

(31) Guimarães, C. R. W.; Bicca de Alencastro, R. Evaluating the Relative Free Energy of Hydration of New Thrombin Inhibitor Candidates Using the Finite Difference Thermodynamic Integration (FDTI) Method. *Int. J. Quantum Chem.* **2001**, *85*, 713−726.

(32) Dauber-Osguthorpe, P.; Roberts, V. A.; Osguthorpe, D. J.; Wolff, J.; Genest, M.; Hagler, A. T. Structure and Energetics of Ligand Binding to Proteins: E. coli Dihydrofolate reductase-Trimethroprim, a Drug-Receptor System. *Proteins: Struct., Funct., Genet.* **1988**, *4*, 31−47.

(33) MacKerell, A. D.; Bashford, D.; Bellott, M.; Dunbrack, R. L.; Evanseck, J. D.; Field, M. J.; Fischer, S.; Gao, J.; Guo, H.; Ha, S.; Joseph-McCarthy, D.; Kuchnir, L.; Kuczera, K.; Lau, F. T. K.; Mattos, C.; Michnick, S.; Ngo, T.; Nguyen, D. T.; Prodhom, B.; Reiher, W. E.; Roux, B.; Schlenkrich, M.; Smith, J. C.; Stote, R.; Straub, J.; Watanabe, M.; Wiorkiewicz-Kuczera, J.; Yin, D.; Karplus, M. All-atom empirical potential for molecular modeling and dynamics studies of proteins. *J. Phys. Chem. B* **1998** *102* (18), 3586−3616.

(34) Hansson, T.; Åqvist, J. Estimation of Binding Free Energies for HIV Proteinase Inhibitors by Molecular Dynamics Simulations. *Protein Eng.* **1995**, *8* (11), 1137−1144.

(35) Jorgensen, W. L.; Blake, J. F.; Buckner, J. K. Free Energy of TIP4P Water and The Free Energies of Hydration of CH₄ and Cl⁻ From Statistical Perturbation Theory. *Chem. Phys.* **1989**, *129*, 193−200.

(36) Åqvist, J. Ion−Water Interaction Potentials Derived from Free Energy Perturbation Simulations. *J. Phys. Chem.* **1990**, *94*, 8021−8024.

(37) Åqvist, J. Modelling of Ion-Ligand Interactions in Solutions and Biomolecules. *J. Mol. Struct. (THEOCHEM)* **1992**, *256*, 135−152.

(38) Essex, J.; Jorgensen, W. L. An Empirical Boundary Potential for Water Droplet Simulations. *J. Comput. Chem.* **1995**, *16* (8), 9510−972.

(39) Press, W. H.; Flanney, B. P.; Teukolsky, S. A.; Vetterling, W. T. In *Numerical Recipes. The Art of Scientific Computing*; Cambridge University Press: CV Cambridge, 1986.

(40) Hockney, R. W. The Potential Calculation and Some Applications. *Methods Comput. Phys.* **1970**, *9*, 136−211.

(41) Woodcock, L. V. Isothermal Molecular Dynamics Calculations for Liquid Salts. *Chem. Phys. Lett.* **1971**, *10*, 257−261.

(42) Berendsen, H. C. J.; Postma, J. P. M.; van Gunsteren, W. F.; DiNola, A.; Haak, J. R. Molecular Dynamics with Coupling to an External Bath. *J. Chem. Phys.* **1984**, *81*, 3684−3690.

(43) Auffinger, P.; Beveridge, D. L. A Simple Test for Evaluating the Truncation Effects in Simulations of Systems Involving Charged Groups. *Chem. Phys. Lett.* **1995**, *234*, 413−415.

(44) Jorgensen, W. L.; Nguyen, T. B. Monte Carlo Simulations of the Hydration of Substituted Benzenes with OPLS Potential Functions. *J. Comput. Chem.* **1993**, *14* (2), 195−205.

(45) Goldblum, A. On the Mechanism of Proteinases. In *Computational Approaches to Biochemical Reactivity;* Náray-Szabó, G., Warshel, A., Eds.; Kluwer Academic Publishers: Dordrecht, 1997; pp 295−340.